

PAPER V

TEIR, S., KUUSIK, R., FOGELHOLM, C.-J., ZEVENHOVEN, R., 2007.
Production of magnesium carbonates from serpentinite for long-term storage of CO₂.
International Journal of Mineral Processing, 85(1-3), 1-15.

© 2007 Elsevier B.V.

Reprinted with permission.

Production of magnesium carbonates from serpentinite for long-term storage of CO₂

Sebastian Teir^{a,*}, Rein Kuusik^b, Carl-Johan Fogelholm^a, Ron Zevenhoven^c

^a Laboratory of Energy Engineering and Environmental Protection, Helsinki University of Technology, P.O. Box. 4400, FIN-02015 TKK, Finland

^b Laboratory of Inorganic Materials, Tallinn University of Technology, Ehitajate tee 5, 19086, Tallinn, Estonia

^c Heat Engineering Laboratory, Åbo Akademi University, Piispankatu 8, FIN-20500 Turku, Finland

Received 8 February 2007; received in revised form 10 August 2007; accepted 26 August 2007

Available online 7 September 2007

Abstract

An approach to capture and storage of CO₂ by precipitation of magnesium carbonate was experimentally studied using aqueous solutions prepared from serpentinite. Serpentinite was first dissolved in 4 M HCl or HNO₃ at 70 °C, after which the excess quantity of solvent was evaporated and the precipitated magnesium salt was mixed with water. CO₂ gas was bubbled through the solution, while the alkalinity of the solutions was controlled using NaOH. A solution pH of 9 was found to be the optimal alkalinity for precipitation of magnesium carbonates from the solution. At this pH, the highest purity of the carbonate product (99 wt.% hydromagnesite), highest amount of CO₂ fixed as carbonate (37 wt.% CO₂ in precipitate), lowest net requirements of NaOH, as well as the highest conversion of magnesium ions to carbonate (94 wt.%) were obtained. Relatively pure iron oxide (88 wt.%) and amorphous silica (82 wt.%) were separated at various stages of the procedure. The high requirements of NaOH (2.4 tonne per tonne CO₂ stored) and make-up acid (2–4 tonne per tonne CO₂ stored) seem to be the largest obstacles to overcome for application of this approach as a CO₂ storage process.

© 2007 Elsevier B.V. All rights reserved.

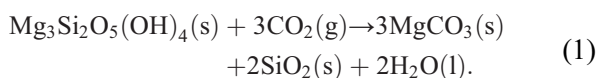
Keywords: Serpentinite; Serpentine; Mineral carbonation; Precipitation; Hydromagnesite; CO₂ capture and storage

1. Introduction

Carbon dioxide capture and storage (CCS) is considered as one of the main options for reducing atmospheric emissions of CO₂ from human activities (IPCC, 2005). This concept includes separation and compression of CO₂ from industry and power plants, and transportation of CO₂ to a suitable storage site. Carbonation of natural silicate minerals is an interesting

alternative to underground geological formations for storage of CO₂.

Alkaline-earth oxides, such as magnesium oxide (MgO) and calcium oxide (CaO), are present in large amounts and high concentrations in naturally occurring silicate minerals, such as serpentine and olivine (Goff and Lackner, 1998). Carbonation of these minerals traps CO₂ as environmentally stable solid carbonates, which would provide storage capacity on a geological time scale. Carbonation of serpentine mineral can be described with the following overall chemical reaction:



* Corresponding author. Tel.: +358 9 4513631; fax: +358 9 4513618.

E-mail address: sebastian.teir@tkk.fi (S. Teir).

The natural carbonation of silicate minerals is very slow, which means that the carbonation reaction must be accelerated considerably to be a viable large-scale storage method for captured CO₂.

In Finland, no geological formations suitable for CO₂ storage seem to exist, but ultramafic rocks, potentially suitable for carbonation, are in some areas fairly common rock types. Serpentinites, consisting mainly of serpentine, are the most interesting of these rocks for CCS purposes. The known and accessible resources of serpentine in Eastern Finland alone could theoretically be sufficient for 200–300 years of CCS processing, if 10 Mt CO₂ per year is stored (Aatos et al., 2006). Serpentinites are already being mined simultaneously with industrial minerals and metals (such as talc, soapstone, chromium, nickel, gold and copper), after which they are piled as barren rock or dammed as tailings.

The most comprehensively studied process for carbonation is an aqueous carbonation process. Although 40–92% conversions can be achieved (depending on the mineral used), the process demands high CO₂ pressures (40–150 bar) and energy for pre-treatment of the mineral. The current estimated cost for such a process is 50–100 US\$/tCO₂ stored (O'Connor et al., 2005), excluding costs for capture, compression and transportation of CO₂. Serpentinites are an important source of a variety of metals and mineral products, making integration of a carbonation process with mineral/metal production a more feasible approach. However, in the aqueous carbonation process, carbonation takes place in a single step by pressurised CO₂ gas reacting with a slurry suspension of magnesium- or calcium silicate, making extraction of minerals or metals difficult. Simultaneous extraction of valuable metals or minerals would require a multi-step carbonation process, which could allow for separation of metals and minerals from serpentine at a process stage prior to carbonation.

Multi-step processes suggested for aqueous carbonation involve leaching or dissolution of silicates in liquid media and precipitation of the dissolved magnesium, or calcium, as carbonates, or hydroxides for subsequent carbonation (IPCC, 2005). Mineral acids (Lackner et al., 1995; Park et al., 2003; Maroto-Valer et al., 2005), organic acids and ligands (Park et al., 2003), as well as caustic soda (Blencoe et al., 2004) have been suggested for dissolving serpentine for subsequent carbonation. In previous work, we found that acids were much more efficient at leaching magnesium from serpentine than bases were (Teir et al., 2007). However, CO₂ dissolves poorly in acidic solutions, and to favour the formation of carbonate ions (and, subsequently, precipitation of

carbonates) the pH of the solution must be raised (Park and Fan, 2004).

In this paper, we have investigated and demonstrated the precipitation of magnesium carbonates from magnesium-rich solutions, prepared from serpentine. After leaching serpentine in aqueous solutions of nitric acid or hydrochloric acid at 70 °C, the solutions were evaporated in order to recycle the acids for reuse. Evaporation of the solutions precipitated a magnesium-rich salt, which was subsequently dissolved in water. These solutions were used for determining the optimal pH for fixation of CO₂ by precipitation of magnesium carbonates at 30 °C in a CO₂ atmosphere of 1 atm.

2. Methods

2.1. Characterisation of serpentine

Serpentine rock from the stockpile of the Hitura nickel mine of Outokumpu Mining Oy, central Finland, was selected for the study. A batch of 7 kg of serpentine rocks was ground to a median diameter of 0.1 mm (size distribution 0–0.5 mm) and analysed using X-ray Diffraction (XRD), X-ray Fluorescence Spectroscopy (XRF) and SEM–SEI (Scanning Electron Microscopy–Secondary Electron Image mode, using a Jeol JSM-840A). X-ray line scan and mapping was also performed with Energy Dispersive X-ray Spectroscopy (EDS) using a Link Analytical AN10000. For a more accurate measurement of the contents of elements in the serpentine, five samples were completely dissolved using an aqueous solution of HCl, H₃PO₄, and HF, from which surplus HF was eliminated using saturated boric acid (H₃BO₃). These solutions were analysed with Inductively Coupled Plasma-Atomic Emission Spectrometry (ICP-AES) to give more exact concentrations of Mg, Fe, Ca, Al, Ni, Mn, Cr, Cu, Co, and Ba in serpentine. The carbonate (CO₃²⁻) content of serpentine was determined by Total Carbon (TC) analysis using a Leybold-Heraeus CSA2003. Since only inorganic compounds were used in the experiments, the total amount of carbon found in the samples, as measured by TC, was assumed to be in the form of carbonates. To verify this, the carbonate content in four of the precipitate samples (as well as in serpentine) was also measured using a Shimadzu 5000A Total Organic Carbon (TOC) analyser, which gives directly the CO₃²⁻ content of the samples. The loss on ignition (L.O.I.) was determined by heating the sample at 970 °C for 1 h. The standard error for using TC instead of TOC for determining the carbonate content of the samples was calculated to be 2%-units. The BET surface area of the serpentine was measured with a Costech Instruments Sorptometer 1042 using multipoint analysis.

2.2. Preparation of magnesium salt solutions from serpentine

Previous research has shown that mineral acids are suitable solvents for extracting magnesium from serpentine: all

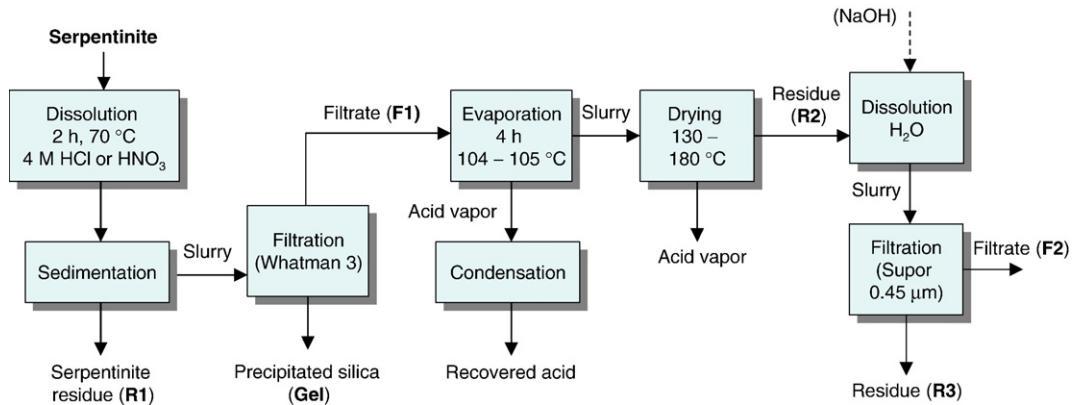
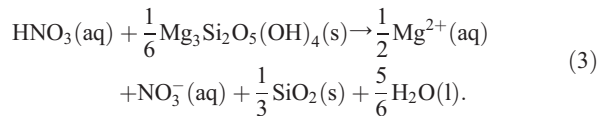
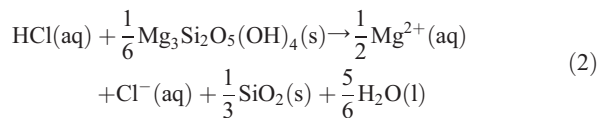


Fig. 1. Overview of the procedure for preparing the solutions used in the precipitation experiments. Sodium hydroxide was only added to the batch prepared from HCl.

magnesium were extracted from serpentine in 1–2 h using 2 M solutions of HCl, HNO₃ or H₂SO₄ at 70 °C (Teir et al., 2007). The chemical equations for extraction of magnesium from serpentine using HCl and HNO₃ are formulated in Eqs. (2) and (3), respectively:



However, in the previous tests (Teir et al., 2007) about six times more acid was used than the stoichiometric requirements

(shown in Eqs. (2) and (3)) in order to maximise the magnesium extraction. One method for recycling excess solvent after extraction could be simple distillation, i.e. evaporation of the solution and condensation of the vapour. However, evaporation requires energy, which could imply additional CO₂ emissions and increase the cost of a carbonation process. A carbonation process using low-temperature heat could be integrated with existing industrial processes and utilise process waste heat. While the boiling point for nitric acid is 83 °C and for hydrochloric acid 48–110 °C (for 38–20 wt.% solutions, respectively), sulphuric acid has a relatively high boiling point of 338 °C. Therefore, sulphuric acid was not used in the experiments. In order to produce magnesium-rich solutions for carbonate precipitation, two batches of salts were prepared from the serpentine; one by dissolving serpentine in HNO₃, and another one by dissolving serpentine in HCl. An overview of the preparation procedure is shown in Fig. 1.

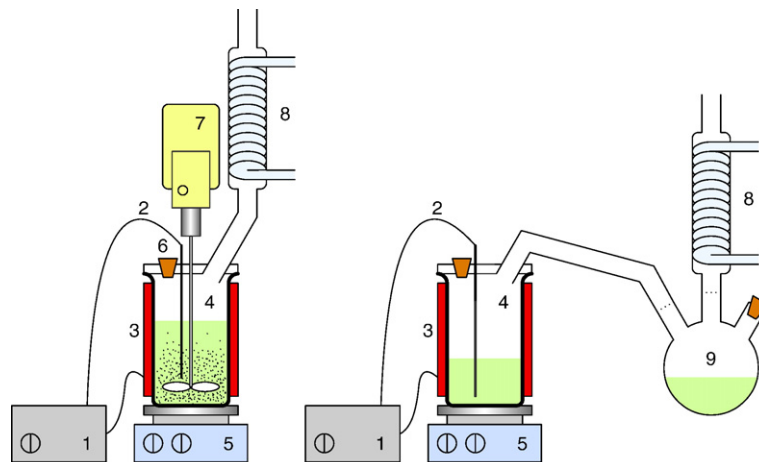


Fig. 2. Setups for dissolving serpentine (left) and preparing magnesium salt (right). 1 — temperature controller; 2 — temperature probe; 3 — electrical heating mantle; 4 — glass reactor; 5 — additional heater; 6 — inlet for feeding solids; 7 — mechanical stirrer; 8 — tap water condenser; 9 — condensate collector flask.

Table 1
Variations in the filtrate preparation procedures

Solvent	V_{F1} (ml)	$T_{\text{evaporation}}$ (°C)	T_{drying} (°C)	t_{drying} (days)	m_{R2} (g)	NaOH ^a added during H ₂ O dissolution (ml)
4 M HNO ₃	928 ^b	104	140–180	2	133 ^c	0
4 M HCl	935 ^b	105	130–140	1	156 ^c	19

^a A solution of 50 wt.% NaOH.

^b A sample of 10 ml was extracted from the listed volume before the solution was boiled.

^c A sample of 7 g was extracted from the listed mass before dissolution in H₂O.

In the first batch, 1 l of 4 M HNO₃ was heated in a glass reactor (2 l) to 70 °C using a temperature-controlled electric element (Fig. 2, left-hand figure). The reactor was equipped with a tap water-cooled condenser to avoid solution vapour from escaping. The solution was stirred at 650 rpm with a mechanical stirrer equipped with a glass propeller. When the temperature had stabilised at 70 °C, 100 g of serpentinite (median diameter of 100 µm) was added to the solution. Two hours after the addition of the serpentinite batch, the solution was removed from the reactor and filtered with a Whatman 3 filter (5 µm). The filtrate (referred to as F1) was transferred to a 2 l glass reactor for evaporation of the solution (Fig. 2, right-hand figure). The reactor was heated with both the electrical heating mantle and the additional heater for evaporating the filtrate. The solution started boiling at 104–105 °C and was boiled for 4 h in order to evaporate most of the solvent. The reactor was connected to another flask (1 l) equipped with a condenser for recovering the evaporated acid (Fig. 2, right-hand figure). After 4 h, 75–80% of the acid solution had been recovered. The residual slurry was dried in an oven for 1–2 days at 130–180 °C for removing as much acid as possible from the slurry. After drying, the residue was cooled to room temperature and dissolved in 2 l H₂O. During dissolution in water a precipitate was formed, after which the solution was filtered through 0.45 µm Pall Supor® membranes. This filtrate (referred to as F2), which had a pH of 7, was used for the precipitation experiments described in Section 2.3.

The second batch was prepared similarly using 1 l of 4 M HCl. The differences in the preparation procedures are listed in Table 1.

The solid residues and products (R1, R2, and R3 in Fig. 1) were sampled and sent for XRF and XRD analysis. The BET surface areas of the solids were also measured (using nitrogen). The residue of serpentinite after leaching in HCl was analysed with SEM–SEI images as well as X-ray line scan and mapping with EDS. The filtrates (F1 and F2) were also sampled and filtered through a 0.45 µm Supor membrane. The dissolved magnesium, iron and silicon concentrations of the solution samples were measured using ICP–AES.

2.3. Precipitation experiments with solutions prepared from serpentinite

The magnesium salt solutions prepared from serpentinite were put in a reactor vessel of 250 or 500 ml, which was heated

up to 30 °C by a water bath (Fig. 3). N₂ gas was introduced to the bottom of a reactor vessel at 1 l/min to ensure a CO₂-free atmosphere in the reactor during heat-up. The solution was continuously stirred at 600–700 rpm by a magnetic stirrer. The reactor was equipped with a condenser to prevent solution losses due to evaporation. The total volume of the working solution was either 150 or 300 ml. A Hanna HI 1131B pH electrode was used for measuring the pH of the solution and the temperature was measured by a PT100 temperature sensor. Both pH and temperature data were stored to a data logger. After the temperature had stabilised at 30 °C, the gas flow was switched to CO₂ (1 l/min). Ten minutes after switching to CO₂ gas (when the pH of the solution had stabilised), the pH was regulated to a specific level by adding drop-wise an aqueous solution of 50 wt.% NaOH. After 30 min of pH regulation, the gas flow was switched back to N₂ (2 l/min) to remove free CO₂ from the reactor. After 15 min under N₂, the prepared solids were collected and washed by filtering through membrane

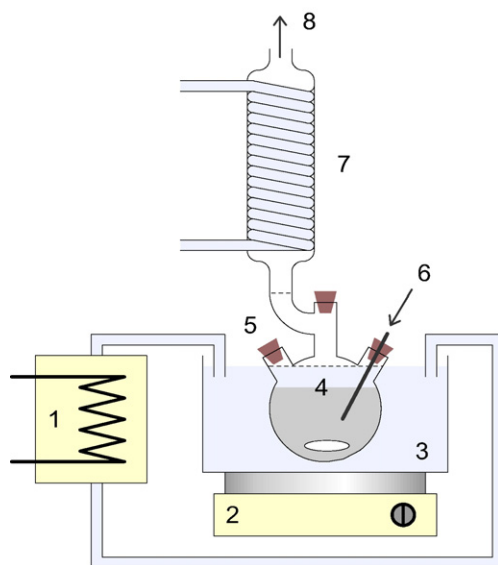


Fig. 3. Experimental rig for precipitation of carbonates. 1 — temperature-controlled bath; 2 — magnetic stirrer; 3 — external bath; 4 — glass reactor; 5 — inlet for NaOH burette; 6 — gas flow in, pH and temperature electrodes; 7 — tap water-cooled condenser; 8 — gas out.

Table 2

Summary^a from XRF analyses (and ICP-AES analyses where indicated) of solids used and produced in the experiments (units: wt.%)

	MgO	SiO ₂	FeO	Al ₂ O ₃	CaO	S	Cr ₂ O ₃	Ni	Cl	MnO	Cu
Serpentinite	40.0	40.3	13.8	0.69	0.53	0.52	0.50	0.28	0.21	0.14	0.08
Serpentinite ^b	36.2	24.8	13.0	0.08	0.48	N/A	0.01	0.02	N/A	<0.01	<0.01
Gel–HNO ₃	4.09	86.7	1.11	0.27	0.02	0.06	<0.01	0.01	<0.01	<0.01	<0.01
R2–HNO ₃	21.6	0.16	2.65	0.06	0.32	0.14	<0.01	0.15	0.03	0.05	0.04
R3–HNO ₃	0.18	1.89	78.9	1.40	0.02	0.72	0.25	>1.1	<0.01	0.98	>0.84
Gel–HCl	3.59	88.2	0.67	0.32	0.02	0.22	0.18	0.14	0.02	<0.01	<0.01
R1–HCl	6.40	82.2	4.03	1.22	0.03	0.49	>1.24	0.22	0.01	0.03	0.02
R2–HCl	13.0	0.44	5.57	0.19	0.62	0.21	0.01	0.10	>35	0.06	0.03
R3–HCl	1.01	1.78	78.2	0.73	0.01	0.24	0.18	>1.1	1.58	0.19	0.50
pH 9–HNO ₃	43.8	0.08	<0.01	0.02	0.50	<0.01	<0.01	0.23	<0.01	0.04	0.01
pH 9–HCl	41.6	0.09	3.36	<0.01	0.21	<0.01	<0.01	0.07	0.02	0.15	<0.01

^a Only elements with concentrations > 0.1 wt.% listed.^b Determined by total acid digestion and ICP-AES analysis. The ICP-AES values listed here are mean values from five similar solutions containing dissolved serpentinite.

filters (Supor 0.45 μm) and dried at 120–135 °C overnight. The composition of the precipitates was analysed using XRF and XRD. The carbon content of the samples was measured by TC analysis and the carbonate content was verified using TOC. SEM–SEI images were used for observing the morphologies of the samples. Experiments were carried out for solution pH 7, 8, 9, 10, 11, and 12 for both salt solutions prepared. The BET surface areas of the solids prepared at pH 9 were measured. One experiment with both solutions was also performed without regulation of pH.

3. Results

3.1. Characterisation of serpentinite

A summary of the results from the ICP-AES, XRD and XRF analyses of the ground serpentinite is shown in Tables 2

and 3. The diffraction pattern and peak list of the XRD run of the serpentinite can be found in Appendix A. The serpentinite consisted mostly of magnesium, iron and silicon in the form of serpentine, (Mg₃Si₂O₅(OH)₄); chrysotile, lizardite and antigorite) and magnetite (Fe₃O₄). Major impurities, according to XRF and TC, were Al, S, Ca, C, Cr, Ni, Cl, Mn, and Cu (concentrations of 0.1–1 wt.%) (Table 2). L.O.I. at 970 °C was 12 wt.%.

The existence of Cr, Cl, and Ca indicates that small amounts of chromite, chlorite and dolomite might be present as well in the sample. Although TOC analysis could not find any traces of carbonate (<0.1 wt.%), the serpentinite contained according to TC analysis 0.2 wt.% carbon. Assuming all this carbon is bound as inorganic carbonates, the serpentinite might contain up to 0.9 wt.% carbonate. Considering that the serpentinite sample also contained 0.5 wt.% CaO, it is likely that C and Ca (as well as a small part of Mg) is bound as dolomite, CaMg(CO₃)₂.

Table 3

Additional analyses of solids used and produced in the experiments

	CO ₃ (wt.%) ^a	CO ₃ (wt.%) ^b	Mass ratio (wt.%) ^c	BET (m ² /g)	Micropore volume (mm ³ /g)	Structural analysis (XRD) ^d
Serpentinite	<0.1	0.875	100%	27.9	2.49	Serpentine (chrysotile, lizardite and antigorite), magnetite
Gel–HNO ₃	N/A	0.90	7%	N/A	N/A	Amorphous, traces of serpentine
R2–HNO ₃	N/A	0.95	134%	N/A	N/A	Magnesium nitrate hydrate, magnesium oxide, magnesium nitride, hydrogen nitrate hydrate
R3–HNO ₃	N/A	0.75	6%	N/A	N/A	Hematite, iron nickel oxide hydroxide
pH 9–HNO ₃	50.2	51.0	64%	27.6	0.00	Hydromagnesite
Gel–HCl	N/A		10%	453	55.1	Amorphous, traces of serpentine
R1–HCl	N/A	0.51	29%	340	40.6	Magnetite, clinocllore, lizardite, amorphous phases
R2–HCl	N/A	0.23	158%	N/A	N/A	Magnesium chloride hydrate, magnesium chloride hydroxide hydrate, traces of iron oxides
R3–HCl	N/A	1.15	10%	110	0.64	Magnetite, goethite
pH 9–HCl	48.4	47.5	61%	29.0	0.38	Hydromagnesite

^a Determined by TOC analysis.^b Calculated using the total carbon content determined by TC analysis, assuming that all carbon is bound as carbonate (CO₃).^c Mass of listed solid per mass of serpentinite used (g solid / g serpentinite).^d Phases listed in apparent descending order of magnitude.

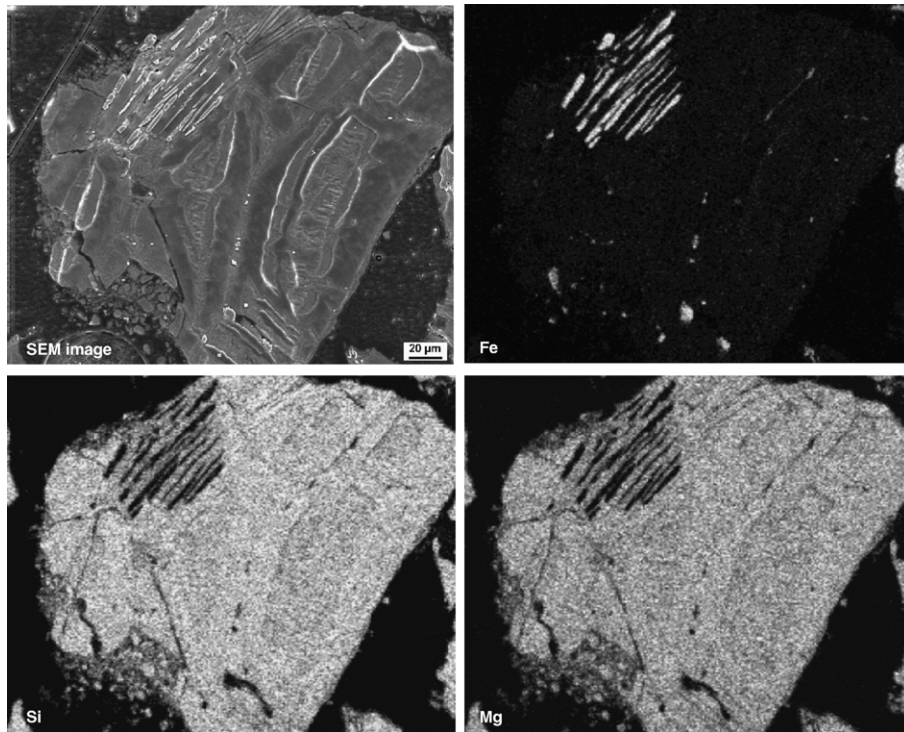


Fig. 4. SEM image and X-ray mapping (EDS) of a cross-section of an untreated serpentine particle.

Some inconsistency was found between the XRF and ICP-AES results (Table 2) regarding the Si content of the sample. Since silica is difficult to dissolve, it is likely that a small part was not dissolved after acid digestion, causing a lower

concentration of Si in the solution measured with ICP-AES. Therefore, the XRF results of the Si content are probably more accurate than the ICP-AES results. However, the opposite should be true for the other elements analysed using both

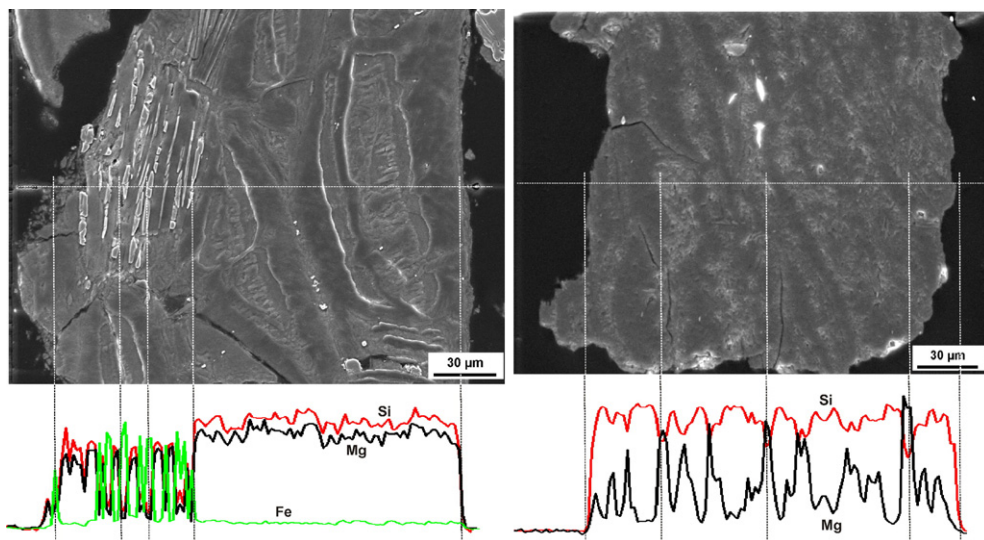


Fig. 5. SEM images and X-ray linescan (EDS) analyses of a cross-section of an untreated serpentine particle (left) and the residue of a serpentine particle leached with HCl (right).

Table 4
ICP-AES analyses of the filtrates from the solution preparations

Solvent	Filtrate F1			Filtrate F2		
	Mg (mg/l)	Fe (mg/l)	Si (mg/l)	Mg (mg/l)	Fe (mg/l)	Si (mg/l)
4 M HNO ₃	20740	4050	14.7	8380	<5	<5
4 M HCl	21580	9400	22.1	8540	810	<5

methods, since the ICP-AES results in Table 2 are mean values of five similarly prepared samples.

Image X-ray mapping (Fig. 4) and line scan (Fig. 5, left-hand picture) with EDS analysis showed that the distribution of magnesium and silicon in the serpentinite particle was relatively homogenous, while iron was located in separate phases. Assuming that all magnesium exist as serpentinite and all iron as magnetite, the composition of serpentinite can be approximated to 83 wt.% serpentinite and 14 wt.% magnetite (based on the magnesium and iron content measured with ICP-AES; Table 2). Since Fe is known to be able to replace Mg in the serpentinite matrix, it is possible that the actual serpentinite mineral content of the serpentinite was slightly higher than 83 wt.%, which would make the actual magnetite content lower than 14 wt.%. Although the relatively high Si content according to the XRF analysis would indicate a serpentinite mineral content significantly higher than 83 wt.%, neither XRD (Appendix A), X-ray mapping (Fig. 4) nor X-ray line scan (Fig. 5, left-hand picture) showed any notable occurrence of Fe in the Si-containing phases of the serpentinite samples that would support this. While better initial equipment choices could have determined a more precise mineralogy of the serpentinite, it was not necessary for the scope of this paper.

3.2. Preparation of magnesium salt solutions from serpentinite

The results from the ICP-AES analyses (Table 4) of the filtrates (F1) showed that dissolution of serpentinite yielded high magnesium and iron concentrations in the solutions, while very little silicon had dissolved. Using the data in Table 2 (ICP-AES data where available), Tables 1 and 4, the conversions of magnesium, iron and silicon in serpentinite to dissolved ions were calculated (Table 5). 88% and 93% of magnesium in serpentinite were extracted using 4 M solutions of HNO₃ and HCl, respectively. Since 100 g of serpentinite was dissolved in 1 l of each solution, over twice (2.2 times) the stoichiometric requirement for acid (Eqs. (2) and (3)) was used (assuming the serpentinite contained 83 wt.% serpentinite). While the choice of solvent had a small effect upon the extraction of magnesium, it had a large effect upon the dissolution of iron: only 37% dissolved during 2 h in 4 M HNO₃, while 87% dissolved in 4 M HCl. The residue of HCl-leached serpentinite (R1–HCl) consisted mostly of silica, but also of magnesium and iron in small concentrations. Both the acid treated residue and the precipitated silica gel had BET

surface areas over ten times that of the untreated serpentinite, and micropores had formed as well (Table 3). Image X-ray mapping (Fig. 6) and line scan (Fig. 5, right-hand picture) with EDS analysis showed that magnesium was inhomogeneously distributed, while silicon was still quite homogeneously distributed. Apparently, magnesium is removed through pores in the silica matrix of serpentinite, leaving amorphous silica in the particle. This is supported by the findings of previous work, where product layer diffusion was found to be the rate limiting step of serpentinite dissolution in HNO₃, HCl and H₂SO₄ (Teir et al., 2007). While most particles of the residue had an inhomogeneous distribution of magnesium (as seen in Fig. 5, right-hand picture), a few singular particles contained separate phases with high levels of magnesium (Fig. 6, particle in the lower left corner of the pictures).

The salt residue (R2–HNO₃) precipitated after evaporation of HNO₃ remained as a red–brown, thick liquid during its residence time in the oven (Table 1), allowing all unreacted acid to evaporate. The precipitate consisted according to XRD and XRF analyses mostly of magnesium nitrate hydrate, Mg(NO₃)₂·6H₂O, but also of amorphous iron oxides (Table 2). The pH of the mixture was roughly 7 after adding H₂O to the residue (R2–HNO₃), allowing all of the iron in the solution to precipitate spontaneously. This was verified by the ICP-AES analyses (Table 4), which found no measurable content of iron in the final filtrate (F2–HNO₃). The iron-rich precipitate (R3–HNO₃) consisted to 88 wt.% of hematite, Fe₂O₃, and contained also enrichments of aluminium, manganese, nickel and copper (Table 2).

When drying the salt residue prepared with HCl, a solid, white crust was formed after one day of drying, while the bottom of the residue remained as a brown liquid. The residue (R2–HCl) contained according to XRD and XRF analyses mostly magnesium chloride hydrate, MgCl₂·6H₂O, and magnesium chloride hydroxide hydrate, Mg(OH)Cl·0.3H₂O, but also traces of iron oxides (Table 2). When dissolving the residue in water, the pH of the resulting clear liquid was equal to 1, preventing iron precipitation. Apparently, the formed crust of magnesium chloride had prevented part of the acid to evaporate. In order to raise the pH to 7 and precipitate iron out from the solution, 19 ml of an aqueous solution of 50 wt.% NaOH was stepwise added during continuous stirring at 1000 rpm (using a magnetic stirrer) for 1 h prior to filtration. However, only 81% of the dissolved iron had precipitated after

Table 5
Conversions of magnesium, iron and silicon in serpentinite to dissolved ions (calculated from the concentration levels in the filtrates with volumes lost due to sampling accounted for)

Filtrate	X _{Mg} (%)	X _{Fe} (%)	X _{Si} (%)
F1–HNO ₃	88.3	37.2	0.1
F2–HNO ₃	88.5	0.0	0.0
F1–HCl	92.6	87.0	0.1
F2–HCl	88.8	18.2	0.0

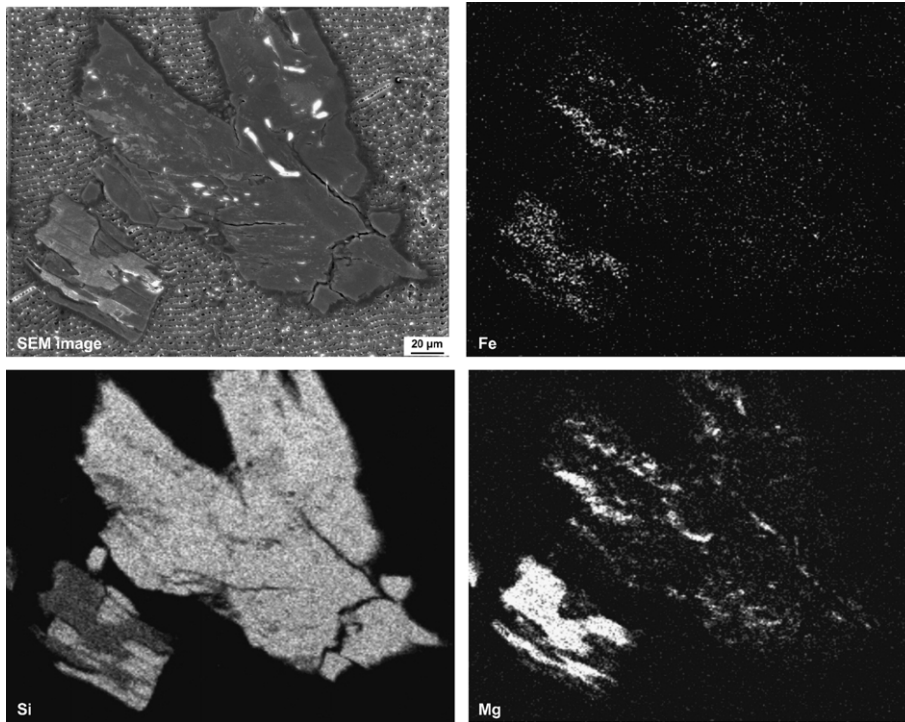


Fig. 6. SEM image and X-ray mapping (EDS) of a cross-section of the residue of a serpentinite particle leached with HCl.

this procedure, which caused the prepared filtrate (F2-HCl) to contain 810 mg/l of iron (Table 4). Part of the magnesium had also precipitated during the procedure, causing the final

filtrate to contain 4% less dissolved magnesium than expected (Tables 4 and 5). The precipitate (R3-HCl) consisted mainly of magnetite, Fe_3O_4 , and some goethite, $\text{Fe}_2\text{O}_3 \cdot \text{H}_2\text{O}$ (Table 3).

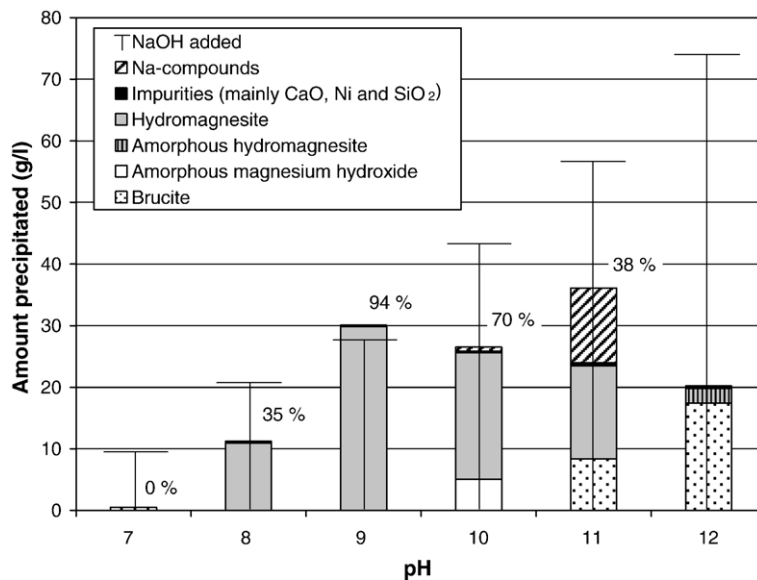


Fig. 7. Formation of precipitate from solutions prepared using HNO_3 by bubbling of CO_2 (1 l/min) and pH regulation by addition of NaOH (50 wt.% in aqueous solution). The conversion of magnesium ions in solution to precipitated hydromagnesite is shown in percentages.

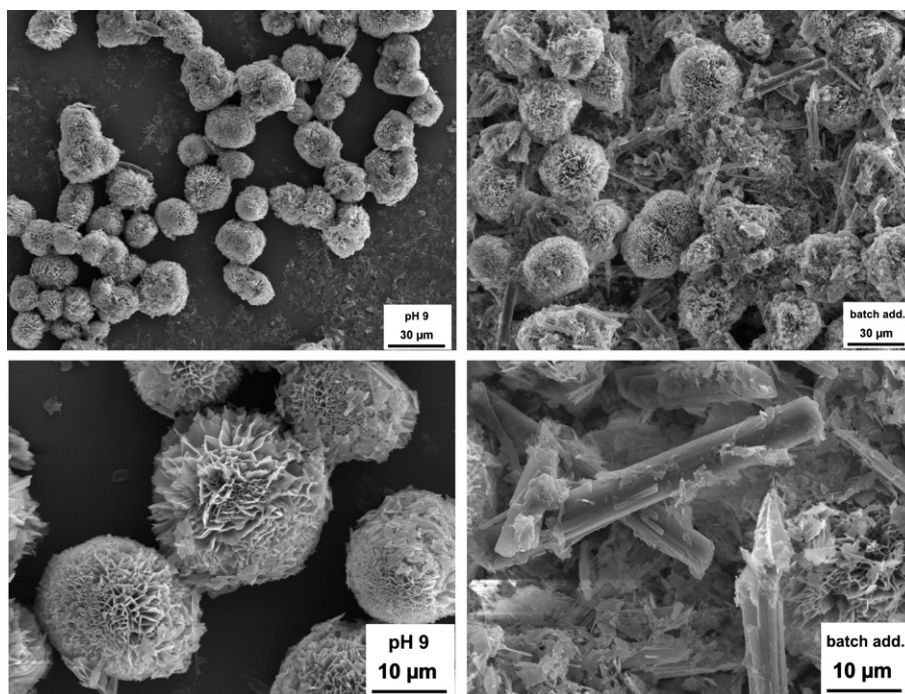


Fig. 8. SEM images of precipitated hydromagnesite from the solution prepared from HNO_3 . Left — precipitate formed by regulating pH at 9 with NaOH. Right — precipitate formed by batch addition of NaOH.

Except for impurities of magnesium oxide, aluminium oxide and silica, a relatively high concentration of nickel was also found in the precipitate (Table 2).

3.3. Precipitation experiments with solutions prepared from serpentinite and HNO_3

When CO_2 was introduced into the solutions at 30 °C the pH dropped from 7 to 5. No precipitate was formed in an initial experiment, which was carried out without any addition of NaOH. Regulating pH to a level between 7 and 12, by addition of NaOH, caused rapid precipitation.

For the solutions prepared using HNO_3 , magnesium precipitated as hydromagnesite, $\text{Mg}_5(\text{CO}_3)_4(\text{OH})_2 \cdot 4\text{H}_2\text{O}$, and brucite, $\text{Mg}(\text{OH})_2$, as well as amorphous hydroxide and carbonate (Fig. 7)¹. Combining the results from XRF and XRD analyses, as well as TC content analyses, the amount of each phase in the precipitates was calculated. Since no sample contained more than one carbonate phase according to XRD, the amount of the identified carbonate phase was estimated based on the carbon concentration measured by TC. The samples, which according to TC contained carbon although no

carbonate phase could be detected by XRD, were assumed to contain amorphous carbonate phases. Depending on the trend of identified magnesite and hydromagnesite phases in the samples produced at lower pH, the amorphous carbonate phases were assumed to be either amorphous magnesite or amorphous hydromagnesite. The amount of magnesium, which could be accounted for neither by the carbonate content nor by detected magnesium hydroxide phases, was accounted for as amorphous magnesium hydroxide. The major part of the precipitated magnesium was bound as carbonates at pH 8–11, with the precipitate produced at pH 9 being pure (99 wt.%) hydromagnesite. The solids, precipitated at pH 9, were measured using TC and TOC to have the highest carbonate content of the precipitates formed: 50 wt.% CO_3^{2-} . At pH 9, the conversion of magnesium ions in solution to hydromagnesite was the highest (94%), while the NaOH requirements were the lowest (0.9 g NaOH/g precipitate). The precipitates formed at pH 9 were uniformly sized, spherical crystals with a lamellar structure (Fig. 8, left-hand photos). Although the SEM images give the impression that the precipitates were highly porous particles, the measured BET surface area was similar to that of the raw material, serpentinite (Table 3).

The experiment performed at pH 9 was repeated by adding the total amount of NaOH required in the previous experiment (0.9 g NaOH/g precipitate) as a batch addition 10 min after the CO_2 flow had been introduced. After the batch addition, the pH was not regulated. The amount of precipitate formed was

¹ The solution formed at pH 11 was difficult to filter, and only one rinse of H_2O was made. Therefore, large amounts of Na-compounds (mostly water-soluble sodium nitrates) existed in the dried solids.

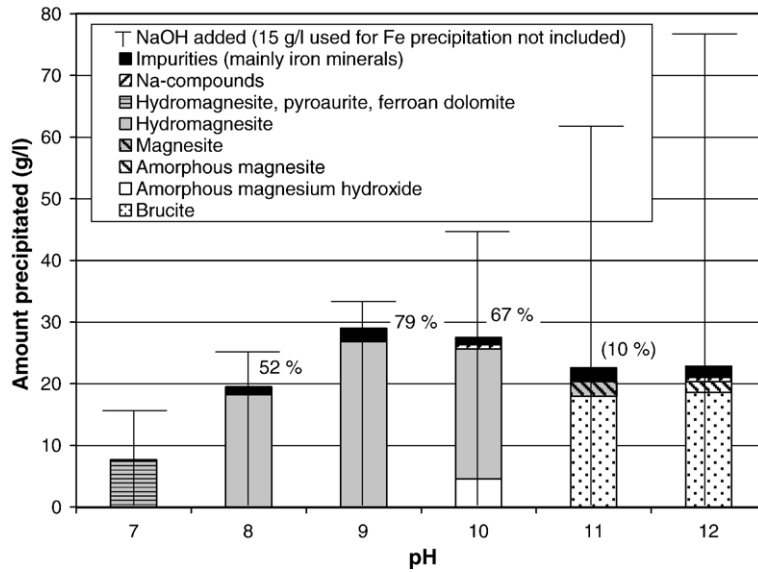


Fig. 9. Formation of precipitate from solutions prepared using HCl by bubbling of CO₂ (1 l/min) and pH regulation by addition of NaOH (50 wt.% in aqueous solution). The conversion of magnesium ions in solution to precipitated hydromagnesite (or magnesite, in brackets) is shown in percentages.

slightly lower (27 g/l solution, 86% conversion), but contained nonetheless pure (99 wt.%) hydromagnesite with a CO₃²⁻ content of 51 wt.%. Although highly crystalline, the precipitates formed after the batch addition of NaOH had more irregular sizes and shapes, with needle-like crystals interconnecting spherical crystals (Fig. 8, right-hand photos).

3.4. Precipitation experiments with solutions prepared from serpentinite and HCl

For the solutions prepared using HCl, magnesium precipitated as hydromagnesite, Mg₅(CO₃)₄(OH)₂·4H₂O, magnesite, MgCO₃, and brucite, Mg(OH)₂, as well as in

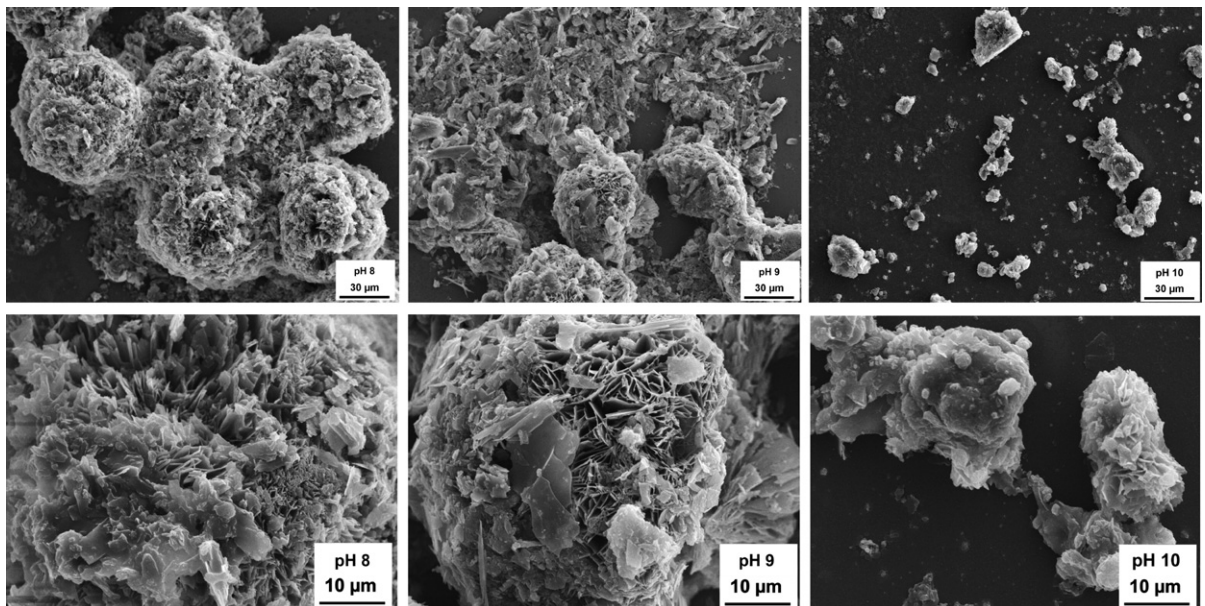


Fig. 10. SEM images of precipitate formed by regulating pH at 8, 9 or 10 using NaOH. The solution used was prepared from HCl and serpentinite.

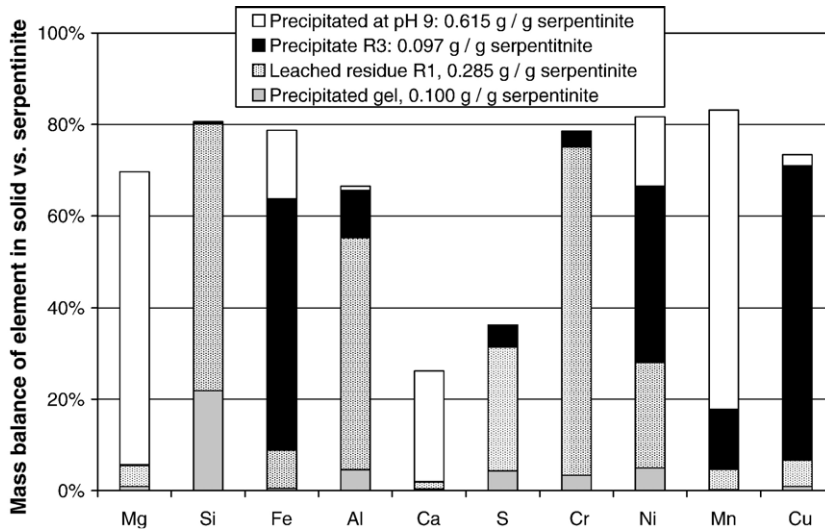


Fig. 11. Mass balance of elements in residue, gel, iron oxide precipitate or carbonate precipitate (prepared using HCl) in relation to serpentinite.

amorphous forms (Fig. 9). However, no precipitate was formed in an initial experiment carried out without NaOH addition. By combining the results from XRF and XRD analyses, as well as carbon content analyses, the amounts of each phase were calculated for most of the precipitates. The amorphous phases were estimated for each sample based on the amount of magnesium and carbonate precipitated in relation to phases identified by XRD. The major part of the precipitated magnesium was bound as carbonates at pH 7–10, with the precipitate produced at pH 9 consisting of 93% hydromagnesite. Since the solution was contaminated with iron, the precipitates produced consisted of 3–9 wt.% Fe. The solids, precipitated at pH 9, were measured using TOC and TC to have the highest carbonate content of the precipitates

formed: 48 wt.% CO_3^{2-} . At pH 9 the conversion of magnesium ions in solution to hydromagnesite was the highest (79%), while the NaOH requirements were the lowest (1.1 g NaOH/g precipitate). As can be seen from the SEM images (Fig. 10) crystals precipitated at higher pH levels were smaller and more compact than those precipitated at lower pH levels. The crystals precipitated at pH 8 were similarly-sized spherical particles with a diameter of 40–60 μm , while those precipitated at pH 9 and pH 10 had more irregular shapes. Both irregularly shaped and needle-like particles were observed at pH 9, while the particles formed at pH 10 were more compact crystals with diameters ranging from 1–100 μm . It is likely that the iron contamination affected the crystallisation of the particles, which may otherwise have had a closer

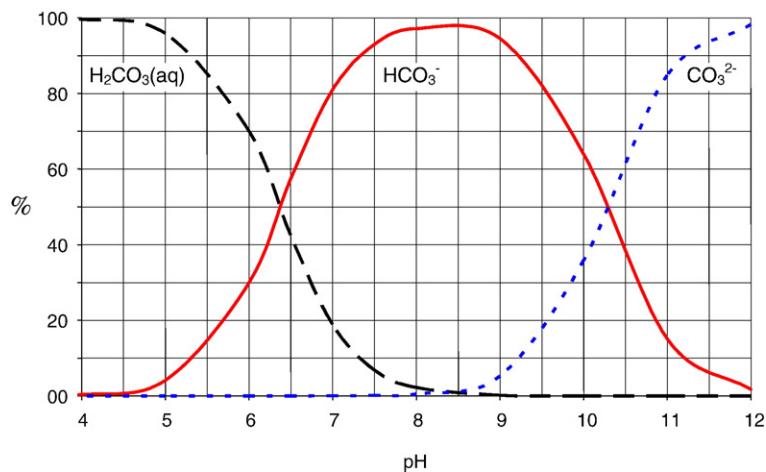


Fig. 12. Distribution of dissolved carbonate species at equilibrium as a function of pH (calculated using Henry's law).

resemblance to those precipitated from the solution prepared using HNO₃ (Fig. 8).

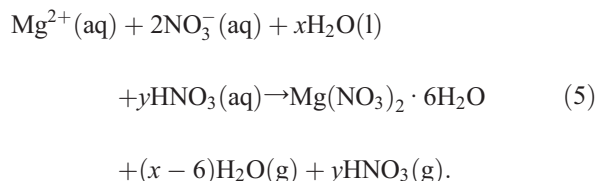
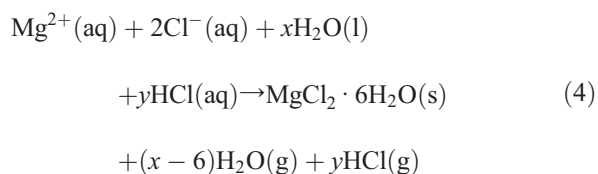
The experiment performed at pH 9 was repeated using a gas mixture of 10 vol.% CO₂ and 90 vol.% N₂ instead of pure CO₂. This time only 6 g precipitate was formed per liter of solution, which is 21% of the amount precipitated using 100% CO₂ gas flow. The precipitate contained mostly pyroaurite, Mg₆Fe₂CO₃(OH)₁₆·4H₂O, with traces of hydromagnesite and brucite. However, the total amount of CO₂ gas fed to the reactor (0.1 l/min during 40 min) was only three times the amount of Mg-ions in solution (Table 4, F2-HCl), while the CO₂/Mg²⁺-ratio in the others experiments was 15–30. A higher gas flow, better gas dispersion, or longer residence time would probably have improved the carbonation.

To examine the distribution of the elements released from serpentinite in various solids formed in the process (with precipitation at pH 9), a mass balance was constructed based on the XRF analyses of the solids (Fig. 11). The mass balance is not complete, since the elements staying in solution after precipitation of carbonate or released as gas were not accounted for. Most of the magnesium in serpentinite ended up in the precipitated carbonate. Using finer grinded material, simultaneous grinding in the dissolution reactor, or a longer dissolution time, more magnesium can be extracted from the serpentinite (Teir et al., 2007; Park and Fan, 2004). A longer reaction time for precipitation might also improve the conversion of dissolved magnesium to hydromagnesite. Most of the copper in serpentinite dissolved in HCl and precipitated together with iron oxide, while most of the chromium (and a large part of aluminium) remained in the serpentinite residue. Most of the calcium is unaccounted for by the mass balance, indicating that most of the calcium remained in solution. Most of the sulphur could not be accounted for, which indicates that sulphur either remains in solution or is released as sulphuric vapours. While most of the silica remained in the leached serpentinite residue, a large part dissolved and precipitated as a gel.

4. Discussion

Both 4 M HCl and 4 M HNO₃ solutions were able to extract most of the magnesium from serpentinite at 70 °C, with HCl dissolving significantly more iron than HNO₃. It appears that magnesium is removed through pores in the silica matrix of serpentine, leaving a highly porous material consisting mostly of amorphous silica. Although a small part of the silica in serpentinite dissolved, it subsequently precipitated due to the high dissolution temperature as a gel and was removed by filtration. While the amorphous silica produced from serpentinite only had a purity of 82–88%, Velinskii and Gusev (2002) reported that it can be refined into 99% pure silica using ultrasonic and electromagnetic separation as well as calcination.

By evaporating the filtered solvents, magnesium salts (containing 2–4% of iron as oxides) were precipitated²:

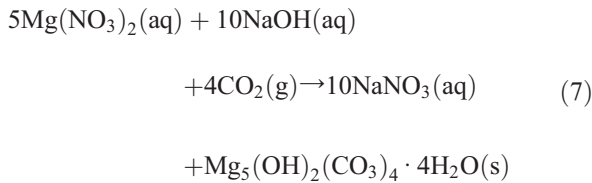
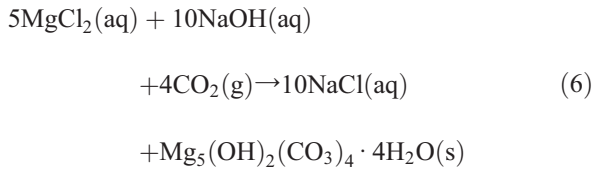


Since part of the solvent used for leaching is converted to magnesium chloride compounds (when using HCl; Eq. (4)), or magnesium nitrate compounds (when using HNO₃; Eq. (5)), only the excess quantity of the solvent can be recycled by evaporation and condensation. Although the chloride- and nitrate contents of the intermediate salts produced were not measured, more than half of the acid used was evaporated at this stage. Since magnesium nitrate has a much lower melting point (89 °C) than magnesium chloride (714 °C) the acid was more easily evaporated from the magnesium nitrate melt than from the magnesium chloride-containing slurry. Part of the acid was not removed from the magnesium chloride-containing slurry, which made the solution formed after adding water very acidic. Adding NaOH to the solution caused most of the dissolved iron to precipitate as magnetite. However, when dissolving the produced magnesium nitrate compounds in water, iron spontaneously precipitated as hematite. The resulting solutions contained very high concentrations of dissolved magnesium and very low levels of impurities, except for iron in the case of the solution produced from HCl. It is possible that the formation of solid magnesium chloride during evaporation of the solvent could be a problem in a large-scale carbonation process, which would favour the use of HNO₃ as a solvent instead of HCl.

In order to precipitate carbonates, the pH of the solutions had to be raised. By adding NaOH simultaneously as CO₂ was bubbled through the solutions,

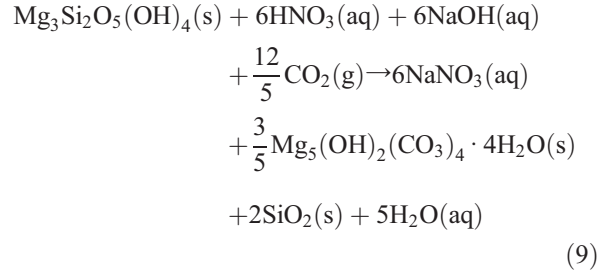
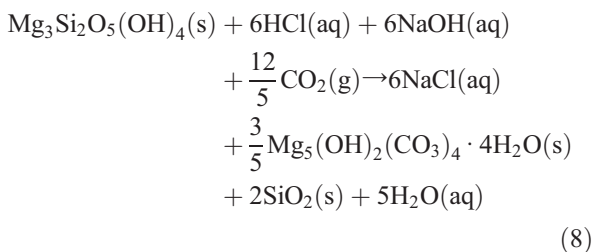
² Only the main chemical reaction, as verified by XRD analysis of the produced salts, is shown in Eqs. (4) and (5).

magnesium precipitated as hydromagnesite at room temperature:



Adding NaOH as a batch seemed to produce almost as much hydromagnesite as adding the same amount of NaOH drop-wise throughout the experiment for controlling the alkalinity of the solution. However, controlling the alkalinity of the solution produced hydromagnesite particles with a more uniform morphology than those produced by batch addition of NaOH. The optimum alkalinity for carbonate precipitation was found to be pH 9, which required 0.9–1.2 g NaOH per gram hydromagnesite produced. This amount is close to the stoichiometric amount (0.86 g NaOH per gram hydromagnesite), assuming that the hydromagnesite precipitation proceeds according to Eqs. (6) and (7). However, the optimal pH level was lower than expected for precipitating carbonates, since calculating the solution equilibrium for carbon dioxide in water shows that carbonate ions are favoured at solution pH higher than 9 (Fig. 12). It is possible that carbonate crystals precipitated at the locations, where the NaOH solution droplets entered the solution. At these spots, the local pH should be temporarily higher than the overall solution pH, until convection distributes the dissolved NaOH evenly.

The net processes for fixation of CO₂ as hydromagnesite using serpentinite are formulated in Eqs. (8) and (9):



At pH 9, the net conversion of serpentinite to hydromagnesite was 70% using HCl and 83% using HNO₃. Using these experimentally verified numbers, about 3.4 t of serpentinite and 2.4 t sodium hydroxide is required per tonne of CO₂ bound as carbonate as 2.7 t of hydromagnesite is produced. Although the concentrations of chloride and nitrate in the waste waters were not measured, the net Eqs. (8) and (9) show that also 2.1 t of HCl or 3.6 t of HNO₃ is consumed per tonne of CO₂ bound. According to TIG (2007), the current price for sodium hydroxide is 180 US\$/t (50% solution), while nitric acid costs 210 US\$/t (price on a 100% basis) and hydrochloric acid costs 72 US\$/t (36% solution). Using these numbers, the costs for make-up chemicals can be estimated to 1300 US\$/t CO₂ (or 480 US\$/t hydromagnesite produced) for a process based on hydrochloric acid and 1600 US\$/t CO₂ (or 600 US\$/t hydromagnesite produced) for a process based on nitric acid. However, it is likely that a cheaper alkaline solution, such as ammonium hydroxide, could be used instead of sodium hydroxide. The current price for ammonia is 180 US\$/t (price on a 100% basis). Using ammonium hydroxide instead of sodium hydroxide, the costs for make-up chemicals would be reduced to 600 US\$/t CO₂ (or 220 US\$/t hydromagnesite produced) for a process based on hydrochloric acid and 940 US\$/t CO₂ (or 350 US\$/t hydromagnesite produced) for a process based on nitric acid.

Elemental mass balances showed that most of the copper in serpentinite precipitated as impurities in the iron oxide, while most of the chromium and aluminium remained in the leached serpentinite residue. The enrichment of copper and chromium in specific solid byproducts may make the recovery of these metals easier. Most of the manganese and calcium in serpentinite precipitated as impurities in the hydromagnesite. Nickel was distributed in all solid byproducts of the carbonation process, which may make the recovery of nickel more difficult.

Production of magnesite, MgCO₃, would allow more CO₂ to be bound per mole magnesium, but the aqueous

environment of the carbonation process seems to favour hydromagnesite formation. Hydromagnesite is less soluble in water (0.4 g/l) than lansfordite, $\text{MgCO}_3 \cdot 5\text{H}_2\text{O}$ (2–4 g/l), or nesquehonite, $\text{MgCO}_3 \cdot 3\text{H}_2\text{O}$ (2 g/l), but more soluble than magnesite, MgCO_3 (0.1 g/l). Hydromagnesite is also thermally stable up to 200 °C. Carbon dioxide is not released from hydromagnesite until the temperature reaches 400 °C (Laoutid et al., 2006). The thermal stability and weak solubility (in water) of hydromagnesite makes it a potential alternative to magnesite for long-term storage of CO_2 . While the produced hydromagnesite may have several industrial applications (e.g. as a fire retardant), the market demand could probably be covered with a small part of the hydromagnesite produced during large-scale CCS processing. The flame retardant markets in the USA and Europe account each for 340 000 tonnes (Weber, 2000). The world production of magnesite was 14.3 Mt in 2005, while the price for synthetic magnesium compounds ranged from 400 US\$/t (for dead-burned magnesia) to 500 US\$/kg (for 100% magnesium hydroxide slurry, technical grade) (USGS, 2005). While the value or possible uses of the synthetic hydromagnesite product, or the other byproducts, is currently not clear, it is possible that selling the products from the carbonation process could compensate for the relatively high process costs. However, if the produced hydromagnesite was to be used as raw materials in processes involving calcination of the magnesite, the stored CO_2 would eventually be released. Therefore, an increased industrial usage of hydromagnesite could have contradicting effects to the initial idea of preventing CO_2 emissions by formation of carbonates.

By using a reactor design that allows for better and longer contact time between gas and solution (e.g. a wet flue gas scrubber) it might be possible to capture CO_2 directly from a flue gas stream with the magnesium-rich, alkaline solution. This approach would remove the need for a separate CO_2 capture unit for separation of CO_2 from the flue gas stream, as well as compression and transportation of CO_2 . However, transportation of minerals would probably be far more energy demanding than transportation of CO_2 , which would require that the flue gas stream is located nearby the source of the minerals.

5. Conclusions

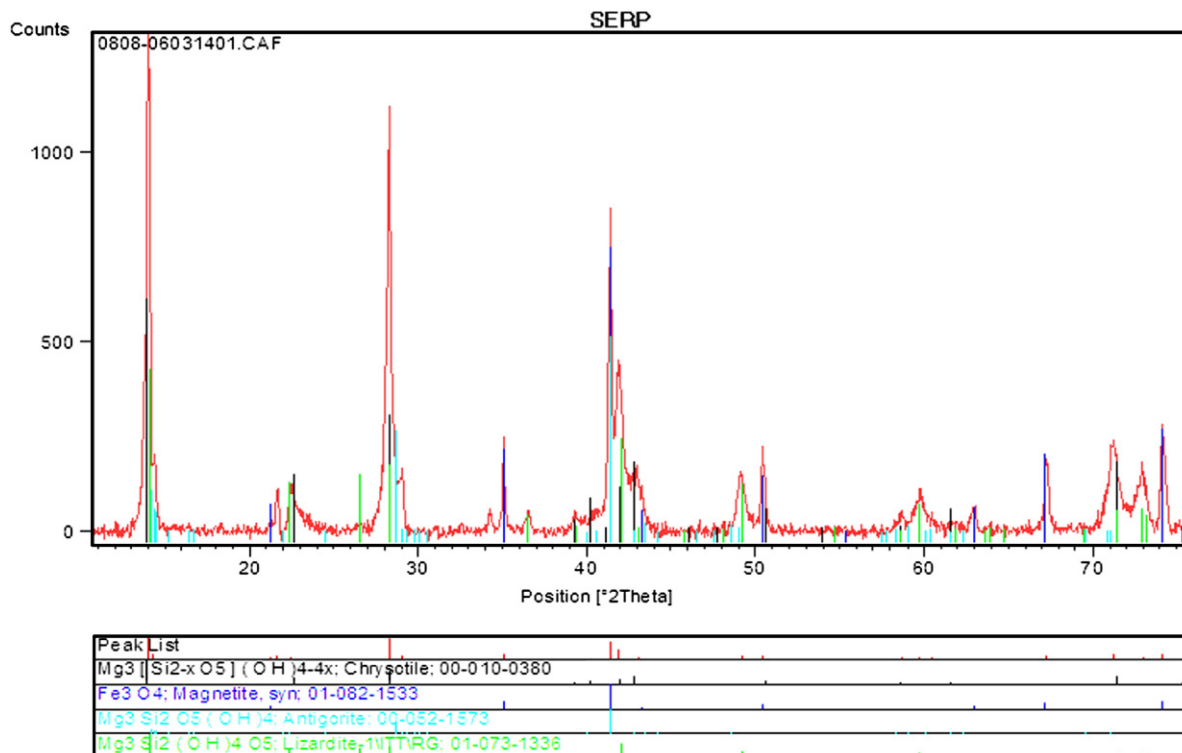
The findings in this paper show that pure hydromagnesite can be produced from serpentinite ore with

a relatively high conversion (80–90%) of serpentinite. At the same time gaseous CO_2 is converted into a solid carbonate. Also, amorphous silica and iron oxides can be separated at various process stages with little effort. Preliminary investigations indicate that the process approach may also be suitable for integration with recovery of copper and chromium. On the other hand, the dispersion of nickel in several byproducts may make the process unsuitable for simultaneous nickel recovery, unless nickel can be recovered before the carbonation processing. While excess acid can be recycled by distillation, the part of the acid that is converted to intermediate salt products is spent in the process. Large amounts of sodium hydroxide are also required for the precipitation step. Since the cost for make-up chemicals alone (600–1600 US\$/t CO_2) is much more than the price for CO_2 emission allowances (1–30 €/t CO_2), the current process design could only be cost effective if the produced hydromagnesite had a similar value as commercial magnesium oxide-based industrial minerals (400–500 US\$/t CO_2). However, the CO_2 emitted during manufacturing of the chemicals spent in the process would probably be of significant proportions, and should be taken into account in future evaluations of the process. In order to lower the operating costs of the process, options for reducing the need for make-up chemicals need to be investigated. The reusability or means for disposal of the spent solution (rich in sodium nitrates or -chlorides) has not yet been investigated. Therefore, more research is required for process design, process optimisation and integration, life-cycle analysis, as well as recycling of the chemicals involved.

Acknowledgements

We thank our co-workers at Helsinki University of Technology: Sanni Eloneva and Jaakko Savolahti for assistance with the experiments, and Mika Järvinen for helpful comments and proof-reading. We also thank our co-workers at Tallinn Technical University: Mai Uibu and Valdek Mikli for SSA and SEM image analyses, respectively. Finally, we thank Rita Kallio and Juha Kovalainen at Ruukki Production for XRF and XRD analyses, as well as Olli-Pekka Isomäki at Hitura nickel mine of Outokumpu Mining Oy for supplying us with serpentinite. The research was funded by Nordic Energy Research, Finnish Funding Agency for Technology and Innovation (TEKES), and Finnish Recovery Boiler Committee.

Appendix A. XRD analysis of the ground serpentinite used in the experiments



References

- Aatos, S., Sorjonen-Ward, P., Kontinen, A., Kuivasaari, T., 2006. Serpentiinin ja serpentiinin hyötykäyttönäkymiä (Outlooks for utilisation of serpentine and serpentinite). Geological Survey of Finland (GSF), Report No. M10.1/2006/3, Kuopio, Finland.
- Blencoe, J.G., Palmer, D.A., Anovitz, L.M., Beard, J.S., 2004. Carbonation of Metal Silicates for Long-Term CO₂ Sequestration; Patent application WO 2004/094043.
- Goff, F., Lackner, K.S., 1998. Carbon Dioxide Sequestering Using Ultramafic Rocks. *Environ. Geosci.* 5 (3), 89–101.
- IPCC, 2005. IPCC Special Report on Carbon Dioxide Capture and Storage. In: Metz, B., Davidson, O., de Coninck, H.C., Loos, M., Meyer, L.A. (Eds.), Prepared by Working Group III of the of the Intergovernmental Panel on Climate Change. Cambridge University Press, Cambridge.
- Lackner, K.S., Wendt, C.H., Butt, D.P., Joyce, E.L., Sharp, D.H., 1995. Carbon dioxide disposal in carbonate minerals. *Energy* 20 (11), 1153–1170.
- Laoutid, F., Gaudon, P., Taulemesse, J.-M., Lopez Cuesta, J.M., Velasco, J.I., Piechaczyk, A., 2006. Study of hydromagnesite and magnesium hydroxide based fire retardant systems for ethylene-vinyl acetate containing organo-modified montmorillonite. *Polym. Degrad. Stab.* 91, 3074–3082.
- Maroto-Valer, M.M., Zhang, Y., Kuchta, M.E., Andrésen, J.M., Fauth, D.J., 2005. Process for sequestering carbon dioxide and sulphur dioxide. US Patent US2005/0002847.
- O'Connor, W.K., Dahlin, D.C., Rush, G.E., Gerdemann, S.J., Penner, L.R., Nilsen, D.N., 2005. Aqueous Mineral Carbonation. Albany Research Center, Final Report, DOE/ARC-TR-04-002, Albany, New York.
- Park, A.-H.A., Fan, L.-S., 2004. CO₂ mineral sequestration: physically activated dissolution of serpentine and pH swing process. *Chem. Eng. Sci.* 59, 5241–5247.
- Park, A.-H.A., Jadhav, R., Fan, L.-S., 2003. CO₂ mineral sequestration: chemically enhanced aqueous carbonation of serpentine. *Can. J. Chem. Eng.* 81, 885–890.
- Teir, S., Revitzer, H., Eloneva, S., Fogelholm, C.-J., Zevenhoven, R., 2007. Dissolution of natural serpentinite in mineral and organic acids. *Int. J. Miner. Process.* 83 (1–2), 36–46.
- TIG, 2007. Chemical Profiles. The Innovation Group (TIG). Available at: <http://www.the-innovation-group.com/chemprofile.htm> [Accessed 18 May, 2007].
- USGS, 2005. Minerals Yearbook. Metals and minerals, vol. 1. U.S. Geological Survey. Available at: <http://minerals.usgs.gov/minerals/> (Accessed 1 February, 2008).
- Velinskii, V.V., Gusev, G.M., 2002. Production of extra pure silica from serpentinites. *J. Min. Sci.* 38 (4), 402–404.
- Weber, M., 2000. Mineral flame retardants — overview & future trends. *Industrial Minerals*, vol. 389, pp. 19–27.